Top Catal (2017) 60:1054–1061
DOI 10.1007/s11244-017-0808-y

ORIGINAL PAPER

Niobium Based Catalysts for Methyl Oleate Epoxidation Reaction

Rosa Turco[1,2] · Rosa Vitiello[1,2] · Riccardo Tesser[1,2] · Alessandro Vergara[1] · Salvatore Andini[1] · Martino Di Serio[1,2]

Published online: 19 April 2017

Abstract In this paper, nine different catalysts have been used for the epoxidation of methyl oleate with hydrogen peroxide as oxidant. The prepared catalysts were mostly based on supported systems niobia–alumina and niobia–silica. Experimental runs were carried out in a lab-scale reactor, keeping constant operating parameters such as reaction temperature (80 °C) and time (5 h), and molar ratio between oxidant and methyl oleate (equal to 4). Runs aimed at the quantitative evaluation of system conversion, yield and selectivity. Nb_2O_5/SiO_2 were found to be active in epoxidation reaction, in particular the catalyst with intermediate niobia loading (6% w/w) showed very high conversion (77%) even if with a very low selectivity to epoxides (30%). Instead, regarding the system based on Nb_2O_5/Al_2O_3, both better activity and selectivity were reached. In particular, the material containing 12% of Niobia yielded the highest values for conversion (83%) and selectivity (89%). The results have been critically discussed through the outcomes of a deep characterization of the catalytic materials, carried out through porosimetric, X-ray diffraction, ultra violet and visible diffuse reflection, and Raman microscopy analyses. The discussion highlighted the more relevant parameters able to influence the activity of niobia-based catalysts in the methylesters epoxidation.

✉ Martino Di Serio
diserio@unina.it

[1] Dipartimento di Scienze Chimiche, Università degli Studi di Napoli Federico II, Complesso Universitario di Monte Sant'Angelo, 80126 Napoli, Italy

[2] Consorzio Interuniversitario di Reattività Chimica e Catalisi (CIRCC), Via Celso Ulpiani 27, 70126 Bari, Italy

Keywords Niobium catalysts · Epoxidation reaction · Fatty acids methylesters

1 Introduction

Renewable resources and bio-based feedstock may present a valid sustainable alternative to petrochemical sources to satisfy the increasing demand for energy and chemicals. Vegetable oils represent an ideal substitute for the chemical feedstock, due to the possibility to synthesize a wide variety of complex molecular structures, oleochemicals, suitable for the industry [1]. The advantages of oleochemicals can be found in several of the "12 principles of the green chemistry", including the call for the use of renewable feedstock, the minimization of hazard, and the production of substances with as little toxicity as possible. Because of their bio-based nature, the oleochemicals are biodegradable, no toxic and CO_2 neutral, since the CO_2 produced from their degradation may be incorporated into next-year crops. Vegetable oils are one of the cheapest and most abundant biological feedstock available in the world, and they are used as starting materials for the production of plasticizers, adhesive coatings, lubricants, useful polymers and polymer composites [2, 3].

Epoxidized vegetable oils (in particular soybean) and the derivate methyl fatty esters are the example of one of the largest industrial applications in this respect, with an annual production of about 200,000 tons [4]. They are used directly as plasticizers and stabilizers for PVC resins, and can be good substitutes for some phthalates that are banned in EU because of their impact on both health and safety [5]. Moreover, considering the high reactivity of the epoxide groups, the epoxidized vegetable oils also act as raw materials for the production of a variety of chemicals such as

polyoils, alkanolamines, and polymers like polyesters and polyurethane [3].

The most common method used in industry to synthesize epoxidized methyl oleate and soybean oil was the epoxidation with performic acid generated in situ by the reaction of the hydrogen peroxide with formic acid, in presence of a soluble mineral acid as catalyst (e.g. sulphuric acid). However, several drawbacks of this method have been recognized over the years, such as the occurring of side reactions (ring opening and polymerization) caused by the presence of homogeneous acids in the reaction system, and the environmental pollution of the waste acids.

New efficient and environmentally friendly systems, such as the use of alternative oxidants and heterogeneous catalysts, may overcome these limitations. In particular, the use of hydrogen peroxide as oxidant is very attractive, because the water is the only one by-product of the reaction. Until now, several types of heterogeneous catalytic systems were reported as active catalysts for the epoxidation, such as TS-1 [6, 7], TiO_2-SiO_2, Ti-MCM41 [8–10], peroxo phospha-tungstate [11], tungsten-based tetrakis [12], alumina [13, 14], transition metal oxides [15].

Although the titanosilicalite sieves, especially titanium silicalite-1 (TS-1), were widely reported as selective catalysts for epoxidation reaction of a variety of organic substrates with hydrogen peroxide, the use of larger molecules like vegetable oils and methylesters (FAME) was limited by the occurring of mass transfer limitations. These drawbacks were overcome by the modification of the zeolite through a decrease of the crystals size or by the incorporation of intra-crystalline mesoporosity, as reported by Glaser et al. [16].

Recently, many niobium oxide (niobia) based materials (e.g. Nb_2O_5–SiO_2 and Nb_2O_5/SiO_2) were proposed for the epoxidation reaction with hydrogen peroxide, due to the high leaching stability and good water tolerance. In particular, it was demonstrated that the niobia–silica based materials, containing the same amount of Nb_2O_5 and prepared by different synthesis methods, have different catalytic activity in methyl oleate epoxidation with H_2O_2 [17–19]. This singular behavior was ascribed to the presence of different species of niobium (isolated or bulk) depending on the nature of the niobium precursor and the synthesis method. Different methods of synthesis lead to the presence of different structures and surface distribution of active sites (Brønsted and Lewis sites), influencing in this way the activity and selectivity in the epoxidation reaction. Recently, a commercial alumina was reported as an efficient catalyst for the epoxidation of methyl oleate with hydrogen peroxide [13], also in the presence of a large substrate like soybean oil [14].

The aim of this work is to compare the activity of silica- and alumina-supported niobia catalysts in the epoxidation of methyl oleate with hydrogen peroxide. Two series of silica- and alumina-supported materials, with various loadings of Nb_2O_5, were investigated to clarify the relation between their catalytic performance, dependent on the acidic features and structures of niobium species, and the support nature.

2 Experimental

2.1 Catalysts

- In this paper, nine different catalysts have been used for the reaction under investigation.
- Catalysts 1 and 2 were based on a commercial γ-alumina powder (Neutral, Brockamn I, Fluka), either as-received (Al_2O_3) or calcined at 900 °C for 6 h (Al_2O_3 900 °C), respectively.
- Catalysts 3–5 are based on Nb_2O_5/Al_2O_3, as obtained by the impregnation method [20]. They differ for the value of the loaded Nb_2O_5 mass content with respect to the whole catalyst mass, namely 3% (3NbAl), 12% (12NbAl) and 15% (15NbAl), respectively. The impregnation has been carried out using a solution of niobium oxalate in oxalic acid (0.1 M solution) as niobium precursor. Niobium oxalate was obtained from niobium pentoxide (99.99%, Sigma Aldrich), according to the procedure described in [20]. After impregnation, the catalysts were dried at 60 °C for 10 h and then calcined at 900 °C for 6 h.
- Catalyst 6 is a commercial silica powder (SiO_2), supplied by Degussa in form of pellets (Aerolyst 3038) and subsequently ground to <100 μm. Catalysts 7–9 are based on this silica powder. In particular, they were prepared borrowing the procedure already described for Nb_2O_5/Al_2O_3 catalysts, and by substituting alumina with silica. The loaded Nb_2O_5 mass contents were 3% (3NbSi), 6% (6NbSi) and 12% (12NbSi), respectively.

2.2 Methyl Oleate Epoxidation

Methyl oleate epoxidation runs with hydrogen peroxide as oxidant were carried out as follows. A round-bottom glass batch reactor (volume of 50 cm^3) heated with an oil bath was used. The lab-scale reactor was equipped with a condenser, a thermometer and a magnetic bar for vigorous stirring @300 rpm. In a typical experiment, 600 mg of catalyst without any pre-treatment, 20 cm^3 of acetonitrile (99.5%, Sigma Aldrich), 5 g of methyl oleate (technical grade, Sigma Aldrich) and 6.9 g of H_2O_2 (54.9% wt, kindly provided by Solvay) were used. Under these conditions, the molar ratio between oxidant and methyl oleate double bonds is nearly 4. The temperature was kept constant

(80 °C) through solvent refluxing. All reagents and the catalyst were added in one pot at the beginning of the reaction, namely when the temperature reached the design value through solvent refluxing. Each test lasted 5 h.

At the end of each experiment, the solution was separated from the catalyst by decantation, and then analysed to evaluate the iodine number (*I.N.* expressed as grams of I_2 per 100 g of sample) and the oxirane number (*O.N.* expressed as grams of epoxidic oxygen per 100 g of sample) [21, 22]. This allowed to calculate the double bond conversion:

$$C\,(\%) = \frac{[I.N.]_i - [I.N.]_f}{[I.N.]_i} \times 100 \quad (1)$$

and the epoxide yield:

$$Y\,(\%) = \frac{[O.N.]_f \times MW_{I_2}}{[I.N.]_i \times MW_O} \times 100 \quad (2)$$

where the suffixes *i* and *f* stand for initial and final, respectively. The ratio between yield and conversion gave the process selectivity *S* (%). The analytical errors concerning the evaluation of iodine and oxirane numbers were determined through repeated tests. The standard deviation σ and the coefficient of variation *CV* % ratio of the standard deviation to the average value were thus obtained: iodine number, $\sigma = 0.3$, $CV = 0.8\%$; oxirane number, $\sigma = 0.04$, $CV = 0.7\%$.

Leaching of the metal is a key point when a strong oxidant like hydrogen peroxide is used in the oxidation reaction, for this reason leaching of the active species into the liquid phase under the current operating conditions has been verified by removing the catalyst from the reaction mixture by filtration after 150 min from the start of the reaction, and then recording the residual conversion for additional 150 min. For each catalyst, almost no detectable further conversion in the filtrate after removing the catalyst was observed, giving evidence that these materials act as real heterogeneous catalysts.

2.3 Materials Characterization

- Textural characterization of the materials has been carried out through evaluation of specific surface area and total specific pore volume (Sorptomatic 1900, BET method). The samples were pre-treated under vacuum at 180 °C for 6 h up to complete degassing.
- X-ray diffraction (XRD) patterns were collected using a Philips powder diffractometer (5–80°2θ, Cu Kα radiation, 0.02°2θ/s scan rate).
- Ultra violet and visible light diffuse reflection (UV-DRS) spectra were acquired in the 200–450 nm range on a doubled beam Jasco spectrophotometer (barium sulphate, Sigma Aldrich, as reflectance standard).
- Finally, a confocal Raman microscope (Jasco, NRS-3100) was used to collect Raman spectra. The 647 nm line of a water cooled Kr^+ laser (Coherent), 10 mW at the sample, was injected into an integrated Olympus microscope and focused to a spot diameter of approximately 2μm by a 20× objective. A holographic notch filter was used to reject the excitation laser line. Raman scattering was collected by a Peltier-cooled 1024×128 pixel CCD photon detector (Andor DU401BVI).

3 Results and Discussion

Figure 1 shows the values of conversion, yield and selectivity obtained during the epoxidation of methyl oleate, as a function of the catalysts used. As can be seen, when the catalysts based on commercial γ-alumina powder are considered as-received alumina shows larger *C* and *Y* values (72 and 58%, respectively), while the selectivity value was higher (84%) for calcined alumina. Switching to the catalysts based on Nb_2O_5/Al_2O_3, it is seen that the material with intermediate Nb_2O_5 loading (12NbAl) yielded the highest values for *C* (83%), *Y* (74%) and *S* (89%). On the other hand, commercial silica was characterized by rather poor values for the parameters under investigation (22%, 7% and 30% for conversion, yield and selectivity, respectively). Finally, among the Nb_2O_5/SiO_2-based catalysts, the one with intermediate niobia loading shows the best performances in terms of conversion (6NbSi; $C = 77\%$).

Alumina itself showed, under these operating conditions, a good and selective catalytic material for the reaction under investigation, accordingly with earlier works [14]. A comparison of the performances of the alumina catalysts with those obtained for the best niobia-loaded alumina-based material (i.e., 12NbAl), suggests that an appropriate preparation procedure leading to a Nb_2O_5/Al_2O_3-based material is able to even improve conversion,

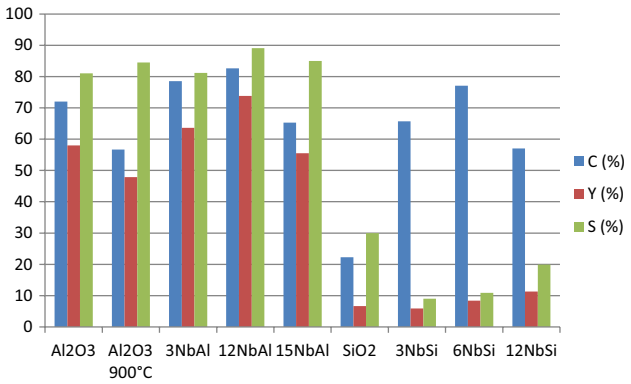

Fig. 1 Values of conversion (*C*), yield (*Y*) and selectivity (*S*) for methyl oleate epoxidation runs carried out with different catalysts

Table 1 BET specific surface area (S_{BET}) and total specific pore volume (V_{TOT}) for the 9 catalysts

Catalyst	S_{BET} (m^2/g)	V_{TOT} (cm^3/g)
Al_2O_3	149	0.43
Al_2O_3 900 °C	118	0.37
3NbAl	64	0.33
12NbAl	77	0.41
15NbAl	75	0.40
SiO_2	180	1.11
3NbSi	115	0.70
6NbSi	114	0.72
12NbSi	108	0.67

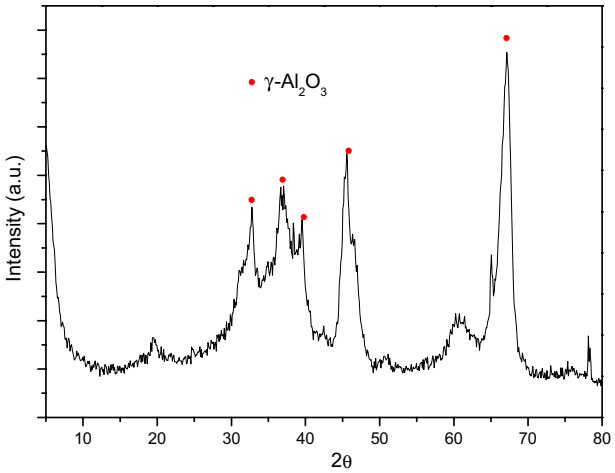

Fig. 2 XRD results for Al_2O_3 900 °C

yield and selectivity. As expected [18, 19], when alumina is substituted by silica in the catalysts synthesis, much worse yield and selectivity values are obtained. Only an in-depth analysis of the main physico-chemical characteristics of the materials at hand would be able to give elements to extend the discussion, in terms of close intertwining between catalysts properties and activity results.

Table 1 lists the values of specific surface area (S_{BET}) and total specific pore volume (V_{TOT}) for the 9 catalysts. Calcination at 900 °C of pure alumina determined the sintering of the material, with a reduction of around 20% and 15% for S_{BET} and V_{TOT}, respectively. Niobia loading on alumina, obviously, resulted into partial closure of the porosimetric texture of the materials, with a non-monotonic trend as Nb_2O_5 loading is increased. The largest values for S_{BET} (77 m^2/g) and V_{TOT} (0.41 cm^3/g) were obtained for 12NbAl. Similar considerations hold when silica-based catalytic materials are considered, but it is seen that silica is both originally more porous and more stable against niobia loading in terms of preservation of the textural characteristics. The effect of the interaction between niobia and alumina could be inferred by looking at earlier papers [23, 24] dealing with an analogous vanadium–alumina system: in our case, the presence of niobium on the alumina surface could promote a thermal instability of the support when high calcination temperatures are used, causing the reduction of catalysts specific surface area.

Figure 2 shows the XRD spectrum for Al_2O_3 900 °C, confirming the presence of γ-alumina (PDF card 10–0425) also after calcination. XRD data for the three catalysts based on alumina and niobia are reported in Fig. 3. It is interesting to observe that: (i) for the material with the lowest niobia loading (3NbAl), no crystalline Nb_2O_5 phase was observed, while γ-alumina was largely predominant; (ii) increasing the Nb_2O_5 loading (12NbAl), the γ-alumina peaks were present together with new signals, related to both Nb_2O_5 (H-monoclin, PDF card 37-1468, and T-orthorhombic, PDF card 30-0873) and non-active $AlNbO_4$ (PDF card 41-0347) phase; (iii) when switching to the material with the largest niobia loading (15NbAl), the peaks relative to $AlNbO_4$ phase seem to be somewhat more relevant. Figure 4 shows the XRD spectra obtained for the three niobia–silica catalysts. While only the hump related to amorphous silica is clearly observable for 3NbSi, when the niobia loading was increased peaks ascribed to Nb_2O_5 (both H-monoclin and T-orthorhombic) were observed [25, 26].

Figure 5a shows the UV-DRS spectra for Al_2O_3 900 °C, pure commercial Nb_2O_5 (calcined at 900 °C), and the three niobia–alumina materials. From the inspection of the figure, it is observed that: (i) Al_2O_3 900 °C has a characteristic signal around 250 nm, while calcined Nb_2O_5 is recognizable from two signals, one around 250 nm and the other one around 350 nm. The former is related to ligand-to-metal charge-transfer (LMCT) transition from O^{2-} to Nb^{5+}. The latter is ascribed to niobia nanodomains, namely slightly distorted NbO_6 octahedra, for example corner-sharing NbO_6 octahedra (confirmed also by Raman spectra); (ii) at the lowest niobia loading (3NbAl), the DRS spectrum of the catalyst was very similar to that of calcined alumina; (iii) at the intermediate niobia loading (12NbAl), the 250 nm-signal related to the presence of niobia appears, while at the highest niobia loading (15NbAl) the other Nb_2O_5 peak (the one related to nanodomains) adds to the DRS spectrum. Figure 5b shows the UV-DRS spectra for SiO_2, Nb_2O_5, and the three niobia–silica catalysts. Once the SiO_2 pattern is taken as a reference, it is observed that the DRS profile for the material at the lowest loading is not very different from that obtained for the silica matrix. On the other hand, 6NbSi and 12NbSi both reflect the presence of Nb_2O_5 with its characteristic signals, the predominant one being that relative to nanodomains, at odds with considerations developed for the niobia–alumina catalysts.

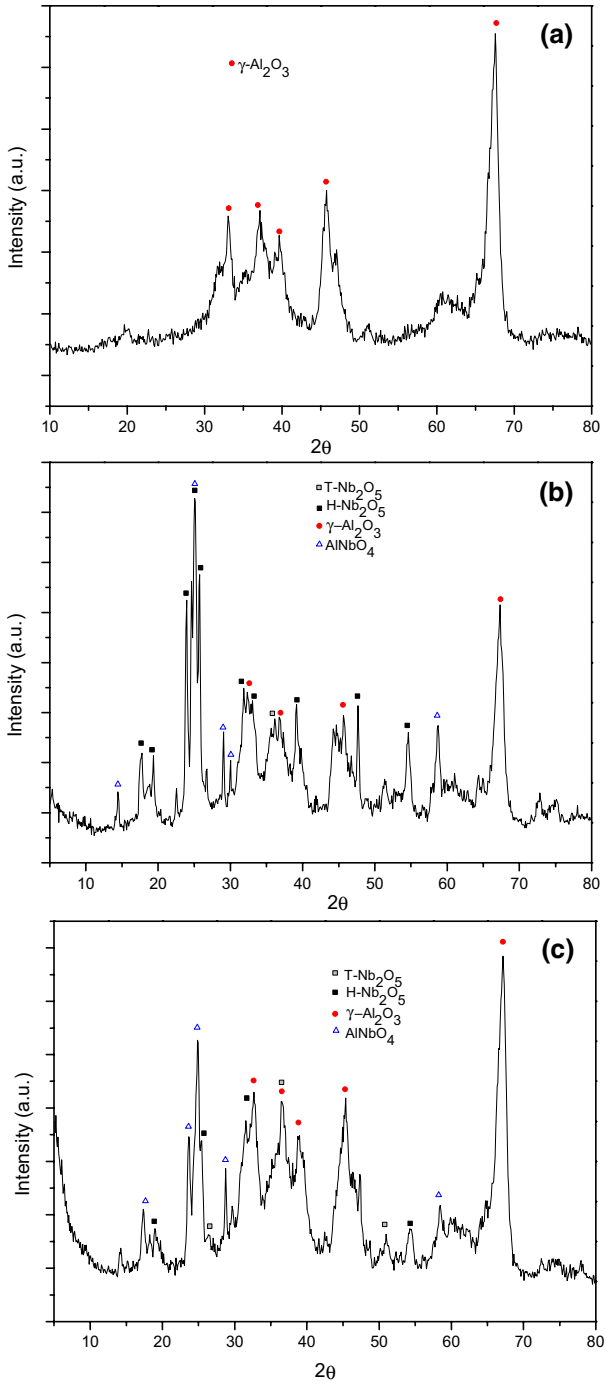

Fig. 3 XRD results for: **a** 3NbAl; **b** 12NbAl; **c** 15NbAl

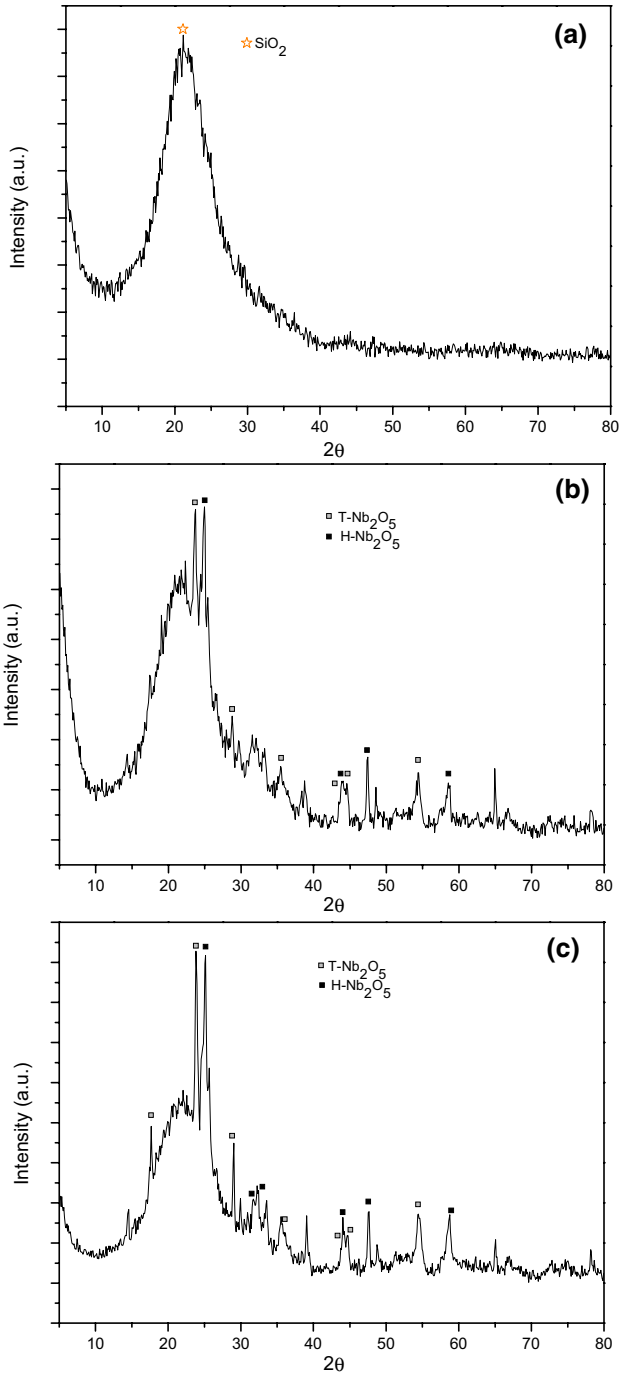

Fig. 4 XRD results for: **a** 3NbSi; **b** 6NbSi; **c** 12NbSi

Namely, Nb coverage of the silica support monolayer with the formation of the related nanodomains is apparent for a lower nominal Nb loading with respect to what occurred when the alumina support was used (6NbSi vs. 15NbAl).

Figure 6 reports Raman spectra for the catalysts which showed (cf. Fig. 1) the best performances, namely those based on niobia and alumina. The reference spectrum for calcined Nb_2O_5 is reported as well. First of all, it is recalled that Jehng and Wachs [27] observed that, for solids based on niobia supported on alumina, slightly and highly distorted NbO_6octahedra appear in the region corresponding to 500–700 and 850–1000 cm^{-1} Raman shift, respectively. Moreover, when the Raman spectrum for calcined Nb_2O_5 is considered, the peak at 995 cm^{-1} is ascribed to Nb_2O_5 bulk, while those at 630 and 675 cm^{-1} to polymerized surface species of metal oxides (corresponding to Brønsted

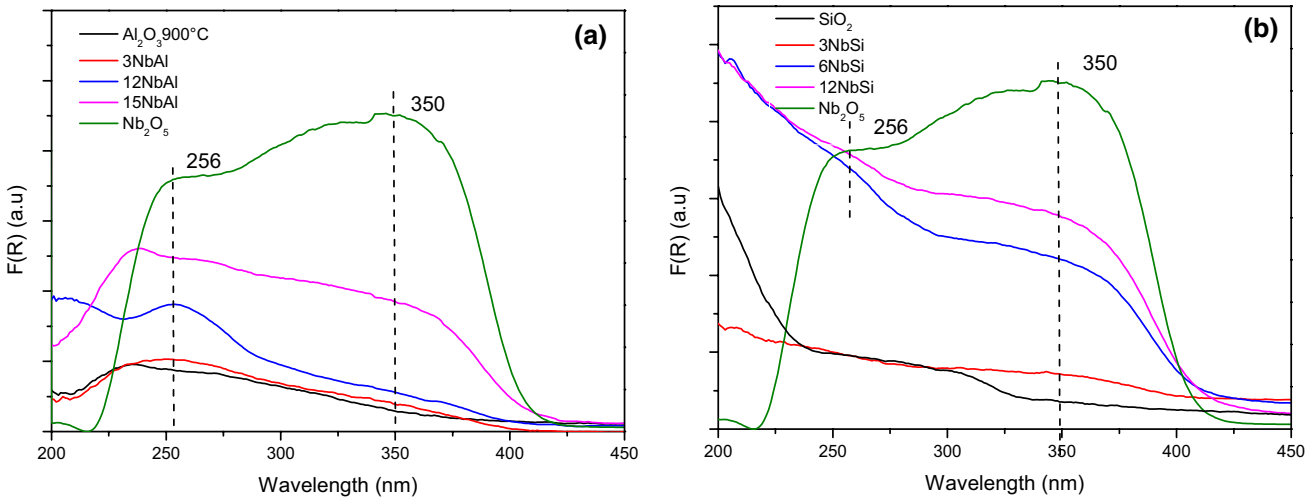

Fig. 5 UV-DRS results for: **a** Al_2O_3 900 °C, pure commercial Nb_2O_5 (calcined at 900 °C), and the three niobia–alumina materials; **b** SiO_2, pure commercial Nb_2O_5 (calcined at 900 °C), and the three niobia–silica materials

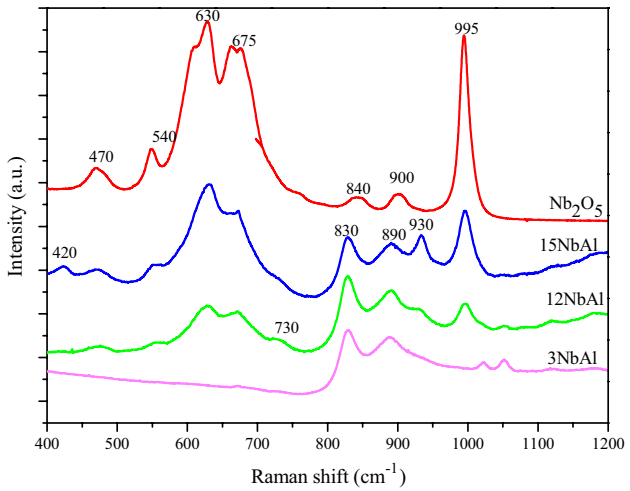

Fig. 6 Raman spectra for pure commercial Nb_2O_5 (calcined at 900 °C) and the three niobia–alumina materials. A 647 nm excitation (10 mW at the sample) was used

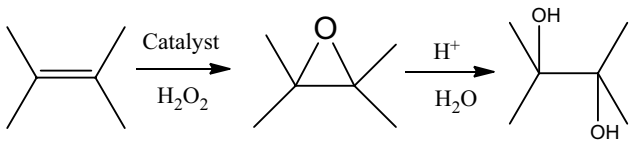

Scheme 1 Epoxidation and ring opening reactions

acid sites). All these signals are present for the catalysts with intermediate (12NbAl) and high (15NbAl) niobia loading, while absent for 3NbAl, somewhat confirming what previously observed by XRD (cf. Fig. 3). It is worth to note that a signal at 930 cm^{-1}, absent for both niobia and 3NbAl spectra, appears as a shoulder for the catalyst with intermediate loading, and as a well-defined band for 15NbAl. This signal is ascribed to $AlNbO_4$ species (cf. XRD data), which has already been recognized as an undesired, since inactivephase [28, 29]. In addition, all the three catalysts are characterized by a band centred at 830 cm^{-1}, associated with highly distorted NbO_6 and corresponding to Lewis acid sites [25].

Two main aspects are recognized from the analysis of the activity results and material characterization, namely a better performance of catalysts (i) based on Nb_2O_5/Al_2O_3 (with respect to those based on Nb_2O_5/SiO_2) and (ii) with intermediate Nb_2O_5 loading (whatever the support). In particular, the best catalyst was 12NbAl (with a performance even better than alumina). The presence of niobia nanodomains, is considered to be detrimental to the catalysts' activity and selectivity. Actually, this implies the presence of Brønsted acid sites that can promote the undesired ring opening reactions with formation of diols (cf. Scheme 1). DRS spectra (cf. Fig. 5) have shown that the formation of niobia nanodomains occur also at low niobium loading for silica support. This unwanted aspect is considered to overtake the better textural characteristics (cf. Table 1) of the catalysts based on silica, when these properties are mirrored in the activity field in terms of conversion, yield and selectivity for the reaction under investigation.

XRD data (cf. Fig. 3) have highlighted the presence of a non-active phase in the epoxidation of methyl oleate (aluminium niobate), whose formation is enhanced when the Nb loading on the support is higher, as also confirmed by Raman spectra (cf. Fig. 6). The better performances obtained for 12NbAl could be thus regarded in the light of the reduced aluminium niobate content (in comparison

with 15NbAl) and larger presence of Lewis acid sites, as witnessed by the 730 cm^{-1} Raman band.

Altogether, in the light of an optimal conduction of the methyl oleate epoxidation in the presence of a catalytic species, the results herein presented highlight the need of a proper characterization of the support and the prepared catalysts, and of taking into account the occurrence of an optimal Nb_2O_5 loading. Actually, increasingly high Nb contents can determine the presence of inactive chemical-physical structures on the support (based on niobium and aluminium), that would eventually lead to decrease the catalysts' activity.

4 Conclusions

The activity of silica- and alumina-supported niobia catalysts in the epoxidation of methyl oleate with hydrogen peroxide was studied. Nb_2O_5/SiO_2-based solids were confirmed to be very active catalysts but not selective towards the epoxidation products. These undesired results were ascribed to the presence of Brønsted acid sites related to polymerized niobia species, observed through XRD and UV-DRS analysis. These sites are responsible of the secondary side-reactions, making this type of catalysts more suitable for diols than epoxides production. Regarding the Nb_2O_5/Al_2O_3-based catalysts, higher activity and better selectivity were reached. The solid with an intermediate loading of Niobia (12%) showed the best performances, also better respect to the bare alumina catalyst, indeed already fairly active for the process under investigation. In fact, larger Nb_2O_5 contents determined the formation of an inactive species, $AlNbO_4$, as confirmed by XRD, UV–Vis DRS and Raman analyses. At low Nb concentration, the interaction of alumina with niobia limits the formation of polymerized niobia species favouring on the contrary the formation of active and selective catalytic site for epoxidation reaction.

Acknowledgements The Authors are grateful to Solvay for having provided hydrogen peroxide. Thanks due to the Finanziamento della Ricerca di Ateneo (000023-ALTRI_DR_3450_2016_Ricerca di Ateneo- CA_BIO) for financial support.

References

1. Schneider MN, Iaconi A, Larocca S (2016) Oleochemical biorefinery. In: Cavani F, Albonetti S, Basile F, Gandini A (eds) Chemicals and fuels from bio-based building blocks. Wiley, Weinheim. doi:10.1002/9783527698202.ch19
2. Meier MAR, Metzger JO, Schubert U (2007) Plant oil renewable resources as green alternatives in polymer science. Chem Soc Rev 36:1788–1802
3. Hill K (2000) Fats and oils as oleochemical raw materials. Pure Appl Chem 72:1255–1264.
4. Bocque M, Voirin C, Lapinte V, Caillol S, Robin JJ (2016) Petro-based and bio-based plasticizers: chemical structures to plasticizing properties. J Polym Sci Part A 54:11–33
5. Turco R, Vitiello R, Russo V, Tesser R, Santacesaria E, Di Serio M (2013) Selective epoxidation of soybean oil with performic acid catalyzed by acidic ionic exchange resins. Green Process Synth 2:427–434.
6. Taramasso M, Perego G, Notari B (1971) U.S. Pat. 1249079.
7. Wilde N, Worch C, Suprun W, Glaser R, (2012) Epoxidation of biodiesel with hydrogen peroxide over Ti-containing silicate catalyst. Microporous Mesoporous Mater 164:182–189.
8. Rios LA, Weckes P, Schuster H, Hoelderich WF (2005) Mesoporous and amorphous Ti–silicas on the epoxidation of vegetable oils. J Catal 232:19–26
9. Campanella A, Baltanas MA, Capel-Sanchez MC, Fierro JLG (2004) Soybean oil epoxidation with hydrogen peroxide using an amorphous Ti/SiO_2 catalyst. Green Chem 6:330–334.
10. Guidotti M, Ravasio N, Psaro R, Gianotti E, Marchese L, Coluccia S (2003) Heterogeneous catalytic epoxidation of fatty acid methyl esters on titanium-grafted silicas. Green Chem 5:421–424.
11. Kozhevnikov IV, Mulder GP, Steverink-de Zoete MC, Oostwal MG (1998) Epoxidation of oleic acid catalyzed by peroxo phosphotungstate in a two-phases ystem. J Mol Catal A 134:223–228
12. Poli E, Clacens JM, Barrault J, Pouilloux Y (2009) Solvent-free selective epoxidation of fatty esters over a tungsten- based catalyst. Catal Today 140:19–22.
13. Sepulveda J, Teixeira S, Schuchardt U (2007) Alumina-catalyzed epoxidation of unsaturated fatty esters with hydrogen peroxide. Appl Catal A 318:213–217
14. Turco R, Pischetola C, Tesser R, Andini S, Di Serio M (2016) New findings on soybean and methylester epoxidation with alumina as the catalyst. RSC Adv 6:31647–31652.
15. Oyama ST (2008) Mechanism in homogeneous and heterogeneous epoxidation catalysis. Elsevier Science, Amsterdam
16. Wilde N, Pelz M, Gebhardt SG, Glaser R, (2015) Highly efficient nano-sized TS-1 with micro-/mesoporosity from desilication and recrystallization for epoxidation of biodiesel with H_2O_2. Green Chem 17:3378–3389.
17. Feliczak A, Walzak K, Wawrzynczak A, Novak I (2009) The use of mesoporous molecular sieves containing niobium for the synthes is of vegetable oil-based products. Catal Today 140:23–29.
18. Di Serio M, Turco R, Pernice P, Aronne A, Sannino F, Santacesaria E (2012) Valuation of Nb_2O_5–SiO_2 catalysts in soybeanoil epoxidation. Catal Today 192:112–116.
19. Turco R, Aronne A, Carniti P, Gervasini A, Minieri L, Pernice P, Tesser R, Vitiello R, Di Serio M (2015) Influence of preparation methods and structure of niobium oxide-based catalysts in the epoxidation reaction. Catal Today 254:99–103.
20. Medeiros F, Moura F, da Silva F, Souza C, Gomes K, Gomes U (2006) The thermal decomposition of monohydrated ammonium oxotris (oxalate) niobate. Braz J Chem Eng 23:531–538
21. Norme Grassi e Derivati NGDC 32 (1976) Stazione Sperimentale Oli e Grassi, ed., Milan, Italy.
22. Paquot C, Hautfenne A (1987) Commission on oils fats and derivatives: standard methods for the analysis of oils, fats and derivatives. Blackwell Scientific Publications, London
23. Jheng JM, Wachs IE (1993) Raman characterization of alumina supported Mo-Ve-Fe catalysts: influence of calcination temperature. J Mol Catal 81:63–75
24. Chary KVR, Kishan G, Kumar CP, Sagar GV (2003) Structure and catalytic properties of vanadium oxide supported on alumina. Appl Catal A 246:335–350

25. Braga VS, Barros ICL, Garcia FAC, Dias SCL, Dias JA (2008) Esterification of acetic acid with alcohols using supported niobium pentoxide on silica-alumina catalysts. Catal Today 133–135:106–112.
26. Kitano T, Shishido T, Teramura K, Tanaka T (2014) Acid property of Nb_2O_5/Al_2O_3 prepared by impregnation method by using niobium oxalate solution: Effect of pH on the structure and acid property. Catal Today 226:97–102.
27. Jheng JM, Wachs IE (1990) The molecular structures and reactivity of supported niobium oxide catalysts. Catal Today 8:37–55.
28. Jheng JM, Wachs IE (1990) Structural chemistry and Raman spectra of niobium oxides. Chem Mater 3:100–107
29. Kitano T, Shishido T, Teramura, Tanaka T (2012) Bronsted acid property of alumina-supported niobium oxide calcined at high temperatures: characterization by acid-catalyzed reactions and spectroscopic methods. J Phys Chem C 116:11615–11625